Performance Analysis of Cool Roof, Green Roof and Thermal Insulation on a Concrete Flat Roof in Tropical Climate

Zingre, Kishor T.
Energy Research Institute at NTU(ERI@N)

Yang, Xingguo
School of Mechanical and Aerospace Engineering, Nanyang Technological University

Wan, Man Pun
School of Mechanical and Aerospace Engineering, Nanyang Technological University

https://doi.org/10.5109/1544078

出版情報：Evergreen. 2 (2), pp.34-43, 2015-09. Green Asia Education Center
バージョン：

Performance Analysis of Cool Roof, Green Roof and Thermal Insulation on a Concrete Flat Roof in Tropical Climate

Kishor T. Zingre[1], Xingguo Yang[2], Man Pun Wan[2,*]

[1]Energy Research Institute at NTU (ERI@N), CleanTech One Singapore 637141

[2]School of Mechanical and Aerospace Engineering, Nanyang Technological University, 50 Nanyang Avenue Singapore, 639798

*Author to whom correspondence should be addressed,

E-mail: mpwan@ntu.edu.sg

(Received August 21, 2015; accepted September 15, 2015)

In the tropics, the earth surface receives abundant solar radiation throughout the year contributing significantly to building heat gain and, thus, cooling demand. An effective method that can curb the heat gains through opaque roof surfaces could provide significant energy savings. This study investigates and compares the effectiveness of various passive cooling techniques including cool roof, green roof and thermal insulation for reducing the heat gain through a flat concrete roof in tropical climate. Computational simulations are performed on a single storey building with 100-mm-thick concrete flat roof. The simulation model is calibrated by measurements conducted in the real building that the simulations modelled after. Simulation results show that a new cool roof reduces net annual heat gain through the roof by about 89-90%, a green roof reduces by about 32-41% and thermal insulation (50-mm-thick polystyrene) reduces by about 62-72%. It means that the annual net heat gain reduction provided by cool roof is the highest among the three passive cooling technologies in the tropical climate. Cool roof enhances heat release from the building whereas green roof and thermal insulation impede building heat release during night time.

Keywords: Cool roof, green roof, thermal insulation, tropical climate, building energy

1. Introduction

The building sector, which accounts for around 40% of the global primary energy consumption, is currently the largest energy use sector in the world [1-3]. Of the energy consumed by buildings, a significant percentage is used by air-conditioning systems to provide comfortable indoor environment [4, 5]. In tropical region where the thermal load of building is heavy, studies show that air-conditioning consumes up to 40-50% in Singapore [6], 40% in Hong Kong [7], and 28% in Taiwan [8] of electricity in buildings. A major source of the thermal load of building is the heat gain from roof [9, 10]. It is suggested by some researchers that roof can contribute up to 50-60% of the total thermal load [11, 12]. Therefore, lessening the heat gain from roof would lead to a considerable reduction of energy consumption, hence mitigation of CO_2 emission and urban heat island (UHI) effect [13, 14].

Roof receives solar radiation during daytime. Part of the radiation is reflected, and the remaining is absorbed. The absorbed energy then is partially lost to outdoor by thermal emission and convection, partially stored in the roof materials, and partially conducted into room [15, 16]. Green roof, cool roof, and insulated roof are three common adopted passive technologies for reducing building heat gain through roofs [17-22]. Nevertheless, they have different work principles and different cooling energy saving performance.

Green roof consists of a layer of soil planted with vegetation above the roof construction. The plants can attenuate the solar radiation before it reaches roof, the soil brings extra insulation, and the moisture in the soil increases the thermal capacity of roof. In addition, evapo-transpiration and evaporative cooling helps release heat from roof [23-25]. Cool roof is usually achieved by either applying a layer of reflective (and emissive) material on the original structural roof or build the roof with reflective (and emissive) construction material. The high solar reflectance reflects more solar energy and the high thermal emittance allows heat to be emitted more effectively. Consequently, less heat is conducted inwards and more heat is released outwards, resulting in less thermal load of the building [26, 27]. Insulated roof uses material with high thermal resistance to construct the roof so to decrease the heat transfer through roof [28, 29]. Compared to green roof and cool roof, insulation is a much more popularly adopted. Many building codes

around the world prescribe *U*-value for roofs for energy efficiency considerations [1, 30, 31].

Studies indicated that the three technologies provide different capacities of energy saving [32-41]. Green roof was reported to be able to attenuate the heat gain of roof by about 60% when the soil is dry with respect to a traditional roofing with an insulating layer, under the weather condition of northeast of Italy [35]. Cool roof could decrease the air conditioning energy consumption by up to 52% for a retail store building in Sacramento, California during summer time [39]. Roof insulation layer can reduce the cooling load by more than 50% for a building compared to uninsulated roof [41]. The studies also suggested that the energy saving benefits of the three technologies would vary when the climate or the condition of original roof changes [32-41]. Simulations were performed for the energy saving benefits of cool roof in 27 cities around the world representing different climates. It was found that after increasing the roof solar reflectance from 0.20 to 0.85, Abu Dhabi observed a saving of 48 kWh/m^2, while Mexico City observed a saving of only 8 kWh/m^2 [38].

Several studies compared the energy saving benefits of these technologies. Kolokotsa et al. [42] found applying cool roof (increased the solar reflectance of roof from 0.20 to 0.89) saved more energy than adding insulation layer (30-mm thick of polystyrene), under the climate of Crete, Greece. Niachou et al. [17] investigated the potential energy saving of different combinations of green roof plus insulation layer under the climate of Athens, Greece, and found that adding green roof could save only 2% of the annual energy of the well-insulated building, while could save up to 31-44% annual energy when the building is non-insulated. Zinzi & Agnoli [25] compared the energy saving benefits of various sets of green roof and cool roof in the Mediterranean region, however, the winter heating penalty occurred in this study suggests that the conclusions may be not applicable to the tropical climate. Up to present, few studies compared all the three technologies in one paper, based on the same primary roof and the same climate, particularly the tropical climate.

To fill this gap, current study investigates the energy saving benefits of the three technologies (green roof, cool roof and thermal insulation) in the tropical climate. A computational study is performed on a real scale building to investigate the energy savings performance of the three technologies in tropical climate.

2. Computational modelling

A single-storey building with a solid flat concrete roof (100-mm-thick concrete + 10-mm-thick plaster on the ceiling) located in Nanyang Technological University, Singapore is used to stage this comparison study. The test building is of rectangular shape having a total opaque roof surface area of about 40 m^2 (without any skylight surface). The test building contains two rooms (as shown in Figure 1): A Store room (whose floor is in contact with air) and a Test room (whose floor is in contact with ground). The Store room has no occupant and is not air conditioned whereas the Test room is occupied and is air conditioned. Two windows, a door and an exhaust fan are located on the south facing wall of the Test room. The Store room has a door on the south facing wall and a window on the west facing wall.

A computational model of the test building is developed using Google SketchUp (version 1.0.7) with OpenStudio plug-in. EnergyPlus [43] programme is used to simulate the heat transfer and energy consumption of the building. Figure 1 shows the three-dimensional model of the test building. Air-conditioning system and internal loads schedules of the Test room are shown in Table A-1 (Appendix). For boundary condition setting, the bottom face of the floor of the Store room is considered as exposed to outdoor air (but not exposed to irradiation). The floor of the Test room is considered as adiabatic and not exposed to any outdoor conditions. The ground temperature input (required by EnergyPlus) is 27^{o}C. Since the Store room has no internal heat load and is not air-conditioned, the results presented in the subsequent sections of this paper (both numerical and experimental) are for the Test room.

The opaque concrete building roof is applied with a cool coating (0.50-mm-thick when dried) having a solar reflectance of 0.74 and thermal emittance of 0.90. The thermo-physical properties of the test building materials are shown in Table 1. The solar reflectance and thermal emittance properties of the cool coating are obtained from on-site measurements (described in Section 3 and Table 4), whereas the thermal conductivity, mass density and specific heat of the cool coating are provided by the building company (CPG Consultants Pte. Ltd.). The Typical Meteorological Year (TMY) weather data file for the Changi airport weather station in Singapore, as summarised in Figure 2, is obtained from the available EnergyPlus weather dataset [44]. Detailed physical and operational information about the test building are shown in Table 2. Simulations are run with three types of roofs, cool roof, green roof and thermal insulation. Details of model setup for each type of roof are explained in Sections 2.1, 2.2 and 2.3. In order to include the shading effect caused by the nearby objects such as buildings, window overhangs and trees, shading elements are utilised, as shown in Table 1. The thermo-physical properties of the building materials which are required as inputs are obtained from the manufacturers and the EnergyPlus material dataset [45] as shown in Table 1.

In this study, green roof, cool roof, and thermal insulation are modelled using the test building. Figure 3 shows the schematic diagrams of the three models.

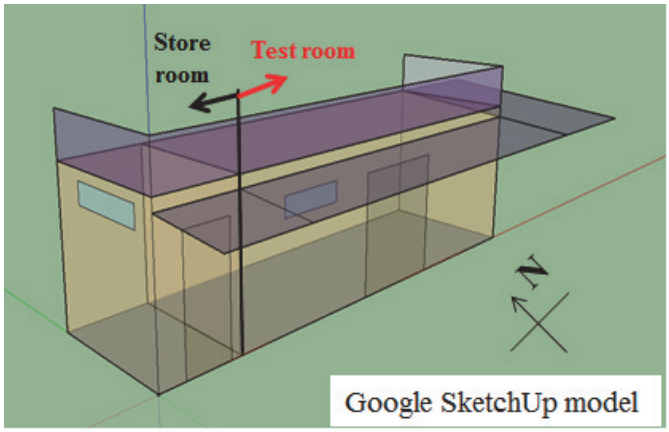

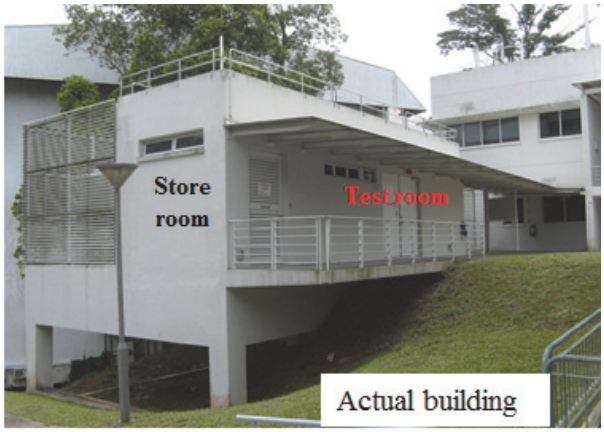

Fig. 1: EnergyPlus (SketchUp) model of the test building.

Table 1: Thermo-physical properties of the test building materials

Building material	Thermal conductivity (W/m-K)	Thickness (mm)	Density (kg/m^3)	Specific heat (J/kg-K)
Air[e+]	0.03	-	1.23	1008
Concrete[e+]	0.65	100[a]	2450	840
Cool coating[a]	0.05[a]	0.5[a]	1053[a]	**
Glazing[e+]	0.70	3.5[a]	-	-
Plastered concrete block[e+]	1.10	125[a]	800	920
Plaster[e+]	0.25	10[a]	850	1000
Wood[e+]	0.15	50[a]	608	1630

[a] Thermo-physical properties are obtained from the manufacturers.

[e+] Thermo-physical properties are taken from the EnergyPlus material dataset [45].

**Thermal mass, m*Cp* is assumed 0 J/K due to negligible mass of coating compared to structural building periphery.

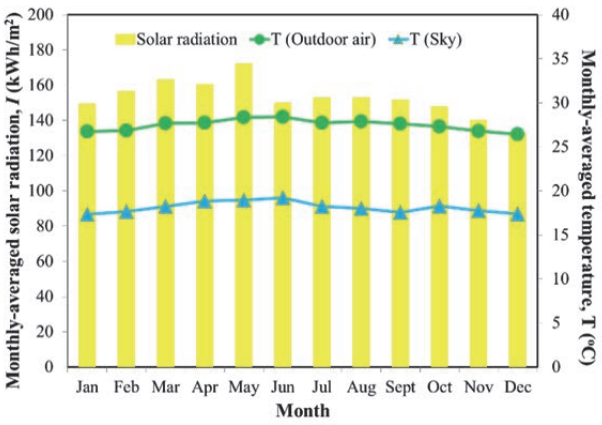

Fig. 2: Typical Meteorological Year weather in Singapore.

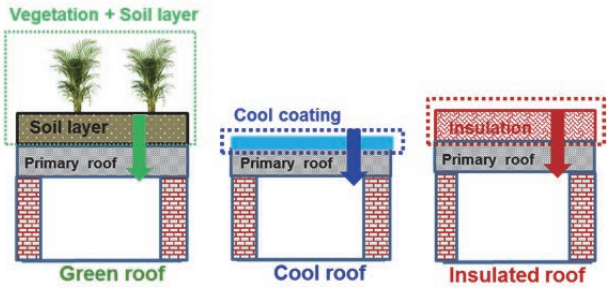

Fig. 3: Schematic diagram illustrating the models of green roof, cool roof, and thermal insulation above target building (not-to-scale).

2.1 Modelling of green roof

EnergyPlus programme features a validated [46] one-dimensional green roof model (Material: Roof Vegetation) which is used to model the effect of green roof in this study. The green roof model [46] takes into account the evapotranspiration of the vegetation layer and evaporation of the soil layer, the transient soil thermal properties and, radiative and convective heat exchanges. Thermo-physical properties of the green roof are shown in Table 2.

2.2 Modelling of cool roof

The effect of the 0.5-mm-thick cool coating layer is modelled in EnergyPlus by assigning the solar reflectance of 0.74 and the thermal emittance of 0.90 of the cool coating and the combined conduction resistance, 0.20 m^2-K/W (adding Conduction resistance of cool coating = 0.19 m^2-K/W and Conduction resistance of concrete = 0.01 m^2-K/W) to the concrete roof. The radiation properties of the cool coating were obtained from the actual measurements on test building roof (as discussed in Section 3).

2.3 Modelling of thermal insulation

Extruded polystyrene insulation, which is commonly employed for the roofs and walls in the tropical region [25], is used as the representative material for thermal

insulation in this study. Thermo-physical properties of extruded polystyrene insulation are shown in Table 3.

Table 2: Thermo-physical properties of green roof [46].

Parameter	Value
Height of plant	0.15 m
Leaf area index	1.2
Leaf solar reflectance	0.10
Leaf thermal emittance	0.86
Minimum stomatal resistance	120 s/m
Max volumetric moisture content of soil	0.32
Min volumetric moisture content of soil	0.01
Initial volumetric moisture content of soil	0.15
Density of soil	960 kg/m^3
Specific heat of soil	1500 J/kg-K
Thermal conductivity of soil	0.4 W/m-K
Soil layer thickness	0.1 m

Table 3: Thermo-physical properties of extruded polystyrene insulation (ASHRAE [47]).

Properties	Value
Thermal conductivity	0.03 W/m-K
Thickness	0.05 m
Density	24 kg/m^3
Specific heat	1590 J/kg-K
Roughness	Medium

2.4 Limitations of the simulation model

EnergyPlus assumes that the air inside a zone is well-mixed and hence has same temperature throughout the zone [43]. The model also assumes that the heat transfer through building envelope surfaces is 1-D [43], ignoring any temperature variation on the same wall/roof surface. These limitations are expected to have minor impact on the accuracy of simulation due to the small size of test building used. Another limitation is that the model cannot account for the transient optical properties (solar reflectance and thermal emittance) of the building surfaces due to aging/weathering effect. These properties are assumed constant in the simulation. However, the current study cannot verify the impact of this limitation since the measurement period only lasted for 1 week which is too short to have any significant aging/weather effect on the building surfaces.

3. Test building measurements for computational model calibration

The computational model developed using EnergyPlus is calibrated by experimental measurements to compare the simulation results for the cool roof surface temperature and the cool ceiling surface temperature with the measurements. The measurements were conducted in the test building for a week in April 2013. Figure 4 illustrates the schematic diagram of the experimental set up.

The cool coating thickness was measured using a coating thickness gauge (Elcometer, A456CSFI1) which was calibrated to an accuracy of ± 1% reading using the zero offset calibration method compatible with ISO 19840 [48]. The cool coating thickness measurements were made at five locations by directly placing the calibrated thickness gauge on the cool coated roof surface.

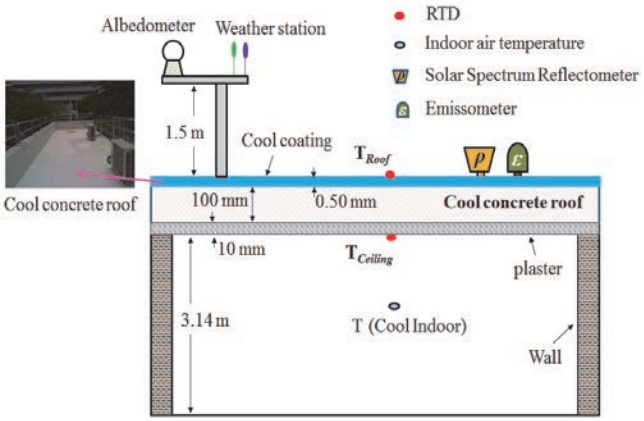

Fig. 4: Schematic diagram illustrating the experimental set up for cool concrete roof of the test building (not-to-scale).

The incident solar radiation received by the roof surface was monitored by an upward-facing (towards the sky) pyranometer (Kipp and Zonen, CMP 11 [49]) mounted at 1.5 m above the roof surface. The pyranometer was factory calibrated to an accuracy of ± 1.4% reading. The detailed calibration procedure of CMP 11 pyranometer can be found in Kipp and Zonen, CMP 11 manual [49]. The surface temperatures of the roof and the ceiling were monitored by surface-type resistance temperature detectors (RTDs) encapsulated in stainless steel probes of 4 mm in diameter and 25 mm in length (Omega, 4 wire RTDs). The calibrated RTDs were installed at five points (to check the homogeneity) of each roof and the ceiling surfaces such that the sensor portion of RTDs was covered with an insulation tape followed by another reflective tape on top. The solar reflectance and thermal emittance properties of the reflective tape were 0.73 ± 0.02 and 0.88 ± 0.02, respectively. These values are almost the same as that of the cool roof (see Table 4). The reflective tape and

insulation tape prevented the sensor tip from being affected by direct solar radiation such that the sensor tip measured the actual temperature of the cool roof surface. The RTDs were calibrated to an accuracy of ± 0.5°C prior to the experiment using a stirred silicon oil bath thermal calibrator (Tempsens Instruments (I) Pvt. Ltd, Calsys -40/200) for the temperature range of 20°C - 40°C (as experienced by the cool concrete roof on a sunny day). The solar reflectance and thermal emittance of both original and cool roof surfaces were measured using a portable Solar Spectrum Reflectometer (Devices and Services, SSR-6) compatible with the ASTM standard C1549 [50] and a portable Emissometer (Devices and Services, AE1-RD1) compatible with the ASTM standard E408 [51], respectively. Both instruments were calibrated using the factory suggested calibration procedures prior to the experiment. The Reflectometer was calibrated to an accuracy of ± 0.001 using the set of calibration standard samples (a black-body cavity, mirror and ceramic tiles) supplied with the instrument. The Emissometer was calibrated to an accuracy of ± 0.01 using the two calibration standard samples, a high thermal emittance standard (ε = 0.88) and a low thermal emittance standard (ε = 0.06), supplied with the instrument. The slide method [50] was used to measure the thermal emittance of the original and cool roof surfaces. In the slide method, the detector head of the calibrated Emissometer was directly placed on the roof surface and allowed about a minute for the detector reading to reach a near steady value. Then the detector was slid several inches across the roof surface to a different spot without breaking contact with the roof surface. Solar reflectance and thermal emittance measurements were made at five locations on the roof surfaces to check the homogeneity. Table 4 summarises the radiation properties of the original and cool roof surfaces.

Inside the test building, at the centre point, a standalone indoor air temperature recorder (MadgeTech, TransiTemp-II [52]) was installed at the height of about 1.6 m above the floor to measure the indoor RH and air temperature. The recorder was factory calibrated to the accuracy of ± 0.5°C temperature and ± 3.5% RH. The detailed specifications and calibration procedure of TransiTemp-II recorder can be found in MadgeTech. TransiTemp-II manual [52]. The outdoor air temperature and wind speed were monitored using a wireless weather station (Scientific Sales Inc., WeatherHawk 916 [53]) installed at the roof of the building. The weather station was factory calibrated to the accuracy of ± 0.5°C temperature and ± 0.3 m/s wind speed. The detailed specifications and calibration procedure of WeatherHawk 916 weather station can be found in Scientific Sales Inc., WeatherHawk 916 manual [53]. Incident solar radiation, surface temperatures, indoor air temperature, outdoor air temperature and wind speed were monitored and recorded at 1-minute intervals. The mass density, specific heat and thermal conductivity of the building materials were obtained from the manufacturers and the EnergyPlus material dataset [45], as shown in Table 1.

Table 4: Radiation properties of the original and cool concrete roof surfaces.

Roof surface	Solar reflectance (ρ)	Thermal emittance (ε)
Original	0.10	0.86
Cool	0.74	0.90

Note: Homogeneity of ρ and ε measurements at five locations was found to be ± 0.02 units.

4. Results

4.1 Computational model calibration

In the test building, the infiltration rate is unknown. In order to obtain a proper infiltration rate, computational simulations are run for the same week in April (during which the test building measurements were conducted) under different infiltration rate settings. Figure 5 shows the matching between measurements and simulation data after calibration.

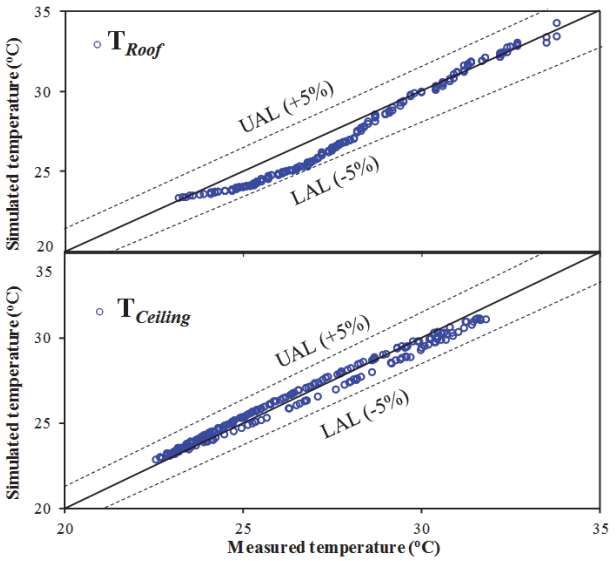

Fig. 5: Comparison of computational simulated temperatures (after calibration) against measured temperatures for the cool roof and cool ceiling. Where, UAL = Upper Acceptable Limit, LAL = Lower Acceptable Limit.

The simulation results obtained under each infiltration rate setting are compared to the measurements results. The roof surface temperature and the ceiling surface temperature are compared in this calibration exercise since these two parameters are used in the subsequent calculation of heat gain through the roof. An infiltration rate of 0.90 air changes per hour (ACH) gives the best matching between simulation and measurement data with errors fall within 5%. The infiltration rate of 0.90 ACH is

used in all subsequent computational simulations. The calibrated model is further used to investigate the effect of solar reflectance and thermal emittance on annual heat gain, annual heat loss and annual net heat gain reduction (as discussed in Section 4.2).

4.2 Effect of cool roof

In this analysis, simulations are performed on an original roof (ε = 0.90, ρ = 0.10), an aged cool roof (ε = 0.90, ρ = 0.55), and a new cool roof (ε = 0.90, ρ = 0.74). The calibrated cool roof model is used for this analysis. Figure 6 shows the annual heat gain, annual heat loss and annual net heat gain (summation of annual heat gain and loss) through the three roofs. The simulations are performed at 3 roof *R*-values covering the common range of roofs (0.48 m^2-K/W to 1.00 m^2-K/W). Table 5 compares the effect of radiation properties on annual net heat transfer.

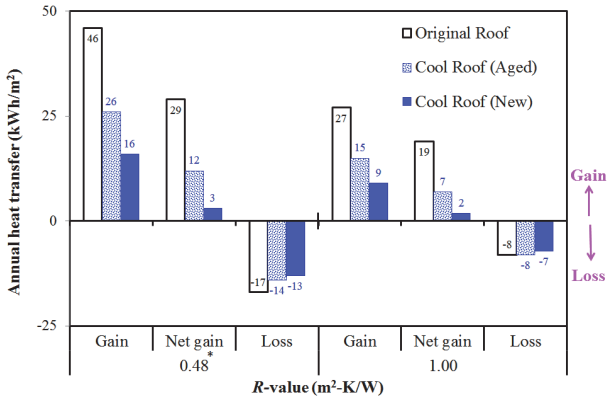

Fig. 6: Comparison of annual heat gain, annual net heat gain and annual heat loss for original roof, aged cool roof, and new cool roof.

Table 5: Comparison of effect of radiation properties on annual net heat transfer.

Reduction	Original roof	Aged cool roof	New cool roof
Annual net heat gain	Reference	59-63%	89-90%
	-	Reference	71-75%

The difference between annual net heat gains for original roof and aged cool roof shows the effect of solar reflectance increment of 0.45 (from 0.10 to 0.55) on annual net heat gain reduction. The difference between annual net heat gain for original roof and new cool roof shows the effect of solar reflectance 0.64 (from 0.10 to 0.74) on annual net heat gain reduction. It can be observed (from Table 5) that the new cool roof provides 90% reduction in annual net heat gain, while the aged cool roof provides 59% reduction in annual net heat gain.

4.3 Effect of green roof

The green roof method provides passive cooling due to two components: 1) conduction resistance offered by the soil layer (about 100-mm-thick) and 2) evapotranspiration by vegetation and evaporation of moisture content in soil. In order to investigate the effect of each component, simulations are performed using the green roof model discussed in Section 2.1. In this analysis, simulations are performed on an original roof and two green roof cases with different leaf area indices (LAI): 1) green roof (LAI = 1), and 2) green roof (LAI = 0.5). In each green roof case, the soil layer is 100-mm-thick, and the thermal emittance of soil layer and vegetation is 0.90. It can be observed (from Fig. 7) that both green roof cases significantly reduce the annual net heat gain as compared to the original roof.

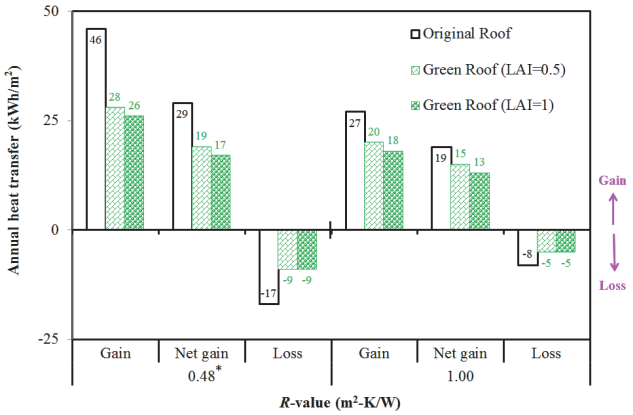

Fig. 7: Comparison of annual heat gain, annual net heat gain and annual heat loss for original roof and green roofs (two cases).

Table 6 compares the effect of green roofs on annual net heat transfer. The comparison between the two green roof cases (for the *R*-value of 0.48 m^2-K/W) shows the effect of LAI alone. The increase in annual net heat gain (due to the decreased LAI of the green roof from 1 to 0.5) is because the decreased leaf area increases the annual heat gain by about 2 kWh/m^2 (or 11%), as can be observed in Fig. 7. However (for the *R*-value of 0.48 m^2-K/W), the annual heat loss remains almost the same (from -9 kWh/m^2 to -9 kWh/m^2). In terms of the annual net heat gain, green roof (LAI = 0.5) is 2 kWh/m^2 (11%) lower than the green roof (LAI = 1). The comparison between original roof and green roof (LAI = 0.5) indicates the effect of conduction resistance due to the soil layer and the shading and evapotranspiration due to the plant. While the comparison between original roof and green roof (LAI = 1) shows the combined effect of conduction resistance and further shading and evapotranspiration.

Table 6: Comparison of effect of green roof on annual net heat transfer.

Reduction	Original roof	Green roof (LAI = 0.5)	Green roof (LAI = 1)
Annual net heat gain	Reference	21-34%	32-41%
	-	Reference	11-13%

4.4 Effect of thermal insulation

Thermal insulation provides additional conduction resistance to the original roof. Extruded polystyrene insulation (25-mm-thick) and extruded polystyrene insulation (50-mm-thick) are simulated (as discussed in 2. 3). In this analysis, simulations are performed on the original roof and the thermal insulation. Figure 8 and Table 7 show the effect of insulation on annual net heat gain reduction through the original roofs.

The comparison between original roof and insulated roof (25-mm-thick) indicates the effect of extra thermal resistance due to the insulation layer. While the comparison between original roof and insulated roof (50-mm-thick) shows the effect of higher extra thermal resistance due to thicker insulation layer.

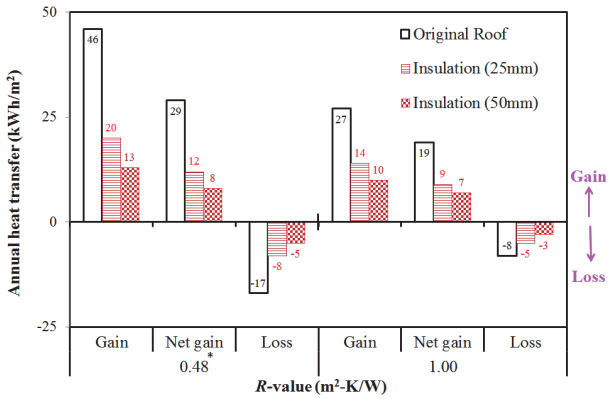

Fig. 8: Comparison of annual heat gain, annual net heat gain and annual heat loss for insulation (50-mm-thick) and original roof.

Table 7: Comparison of effect of insulation on annual net heat transfer.

Reduction	Original roof	Insulation (25-mm-thick)	Insulation (50-mm-thick)
Annual net heat gain	Reference	53-59%	62-72%
		Reference	22-33%

4.5 Comparison between cool roof, green roof and thermal insulation

Figure 9 shows the annual net heat gain reduction due to the increment in solar reflectance (from 0.10 to 0.74) due to the application of new cool roof over original roof, addition of soil layer (100-mm-thick with LAI = 1), and extruded polystyrene insulation (50-mm-thick). Figure 9 also shows the annual net heat gain increment due to the decrease in solar reflectance due to aging of new cool roof (from 0.74 to 0.55). It can be observed (from Fig. 9) that the increment in solar reflectance (by 0.64) provides the highest annual net heat gain reduction (about 89-90%) for all *R*-values. While, the annual net heat gain reduction provided by combined evapotranspiration + soil resistance (green roof with LAI = 1) reduces from 55% to 75%, and by extruded polystyrene insulation (50-mm-thick) reduces from 62% to 72%. This shows that the percentage annual net heat gain reduction provided by the increment in solar reflectance almost remains constant, while that due to increment/addition of conduction resistance and green roof properties decreases with the increase in *R*-value of the roof, as can be observed from Fig. 9. The decrement in solar reflectance from 0.74 to 0.55 (due to the aging of cool roof) results in increase in annual net heat gain by up to 300%.

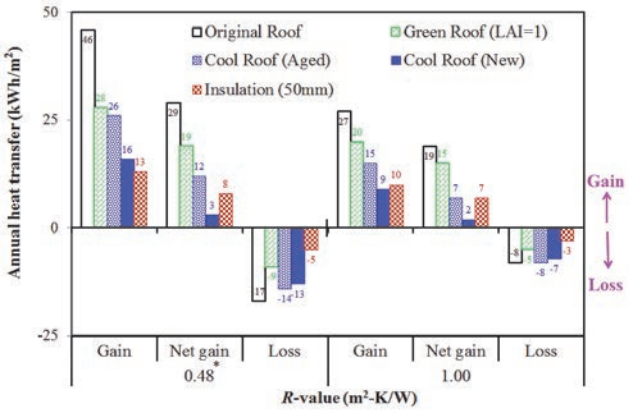

Fig. 9: Annual net heat gain reduction brought by the increment in radiation properties, green roof properties and thermal insulation.

5. Conclusions

The thermal performance of various passive roofing technologies on a flat concrete roof (cool roof, green roof and thermal insulation) is compared by performing computational simulations on an air-conditioned, single-storey building in tropical climate. The computational model was calibrated using experimental measurements. It is found that for the commonly used roofs in tropical climate (*R*-value in the range 0.48 m^2-K/W to 1.00 m^2-K/W), the annual net heat gain reduction provided by

- a new cool roof is about 89% to 90%,
- an aged cool roof is about 59% to 63%,
- a green roof (LAI = 1) is about 32% to 41%, and adding extruded polystyrene insulation (50 mm thick) is about 62% to 72%.

This shows that the annual net heat gain reduction provided by cool roof is highest among the three passive cooling technologies in the tropical climate.

Acknowledgements

This study is supported by MND-A*Star Green Building Joint Grant through grant no. 1121760021. The technical and logistical support by Energy Research Institute at NTU (ERI@N) is greatly appreciated.

Appendix

Table A-1: Air-conditioning system and internal loads of the Test room.

Air-conditioning system	Single Split Type: On[b] / Off[c] Indoor set temperature: 24°C Cooling capacity: 2.5 kW COP: 3.33 Power consumption: 0.75 kW Annual operating hours: 3012 hours
Internal loads	No. of people[b]: 4 No. of people[c]: 0 Lighting level[b]: 432 W Lighting level[c]: 0 W Electric equipment[b]: a desktop (250 W) and an exhaust fan (25 W) Electric equipment[c]: a desktop (0 W) and an exhaust fan (0 W) Ventilation rate: 0.30 ACH Infiltration rate: 0.90 ACH

[b]Schedule during weekday (Monday to Friday) operating hours: 07:00 – 19:00.
[c]Schedule during weekday off hours, weekends (Saturday and Sunday) and holidays.

References

1) Laustsen, J., *Energy efficiency requirements in building codes, energy efficiency policies for new buildings.* International Energy Agency (IEA), 2008: p. 477-488.
2) Eicker, U., *Low energy cooling for sustainable buildings*. 2009: John Wiley & Sons.
3) *Energy Efficiency in Buildings: Lessons Learned from International Experience.* United Nations Development Programme, Energy and Environment Group, New York, USA, 2009.
4) Castleton, H.F., et al., *Green roofs; building energy savings and the potential for retrofit.* Energy and Buildings, 2010. **42**(10): p. 1582-1591.
5) Al-Rabghi, O.M. and M.M. Akyurt, *A survey of energy efficient strategies for effective air conditioning.* Energy Conversion and Management, 2004. **45**(11–12): p. 1643-1654.
6) Kua, H.W. and C.L. Wong, *Analysing the life cycle greenhouse gas emission and energy consumption of a multi-storied commercial building in Singapore from an extended system boundary perspective.* Energy and Buildings, 2012. **51**: p. 6-14.
7) Lam, J.C., et al., *Residential building envelope heat gain and cooling energy requirements.* Energy, 2005. **30**(7): p. 933-951.
8) Lai, C.-m., J.Y. Huang, and J.S. Chiou, *Optimal spacing for double-skin roofs.* Building and Environment, 2008. **43**(10): p. 1749-1754.
9) Hernández-Pérez, I., et al., *Thermal performance of reflective materials applied to exterior building components—A review.* Energy and Buildings, 2014. **80**: p. 81-105.
10) Tong, S., et al., *Thermal performance of concrete-based roofs in tropical climate.* Energy and Buildings, 2014. **76**: p. 392-401.
11) Nahar, N.M., P. Sharma, and M.M. Purohit, *Performance of different passive techniques for cooling of buildings in arid regions.* Building and Environment, 2003. **38**(1): p. 109-116.
12) Nahar, N.M., P. Sharma, and M.M. Purohit, *Studies on solar passive cooling techniques for arid areas.* Energy Conversion and Management, 1999. **40**(1): p. 89-95.
13) Wee, K.F., et al., *Energy consumption and carbon dioxide emission considerations in the urban planning process in Malaysia.* 2008.
14) Xu, T., et al., *Quantifying the direct benefits of cool roofs in an urban setting: Reduced cooling energy use and lowered greenhouse gas emissions.* Building and Environment, 2012. **48**(0): p. 1-6.
15) Reagan, J.A. and D.M. Acklam, *Solar reflectivity of common building materials and its influence on the roof heat gain of typical southwestern U.S.A. residences.* Energy and Buildings, 1979. **2**(3): p. 237-248.
16) Zingre, K.T., et al., *Modeling of cool roof heat transfer in tropical climate.* Renewable Energy, 2015. **75**: p. 210-223.
17) Niachou, A., et al., *Analysis of the green roof thermal properties and investigation of its energy performance.* Energy and Buildings, 2001. **33**(7): p. 719-729.
18) Santamouris, M., et al., *Investigating and analysing the energy and environmental performance of an experimental green roof system installed in a nursery school building in Athens, Greece.* Energy, 2007. **32**(9): p. 1781-1788.
19) Kolokotroni, M., B.L. Gowreesunker, and R. Giridharan, *Cool roof technology in London: An experimental and modelling study.* Energy and Buildings, 2013. **67**: p. 658-667.
20) Romeo, C. and M. Zinzi, *Impact of a cool roof application on the energy and comfort performance*

in an existing non-residential building. A Sicilian case study. Energy and Buildings, 2013. **67**: p. 647-657.
21) Mohsen, M.S. and B.A. Akash, *Some prospects of energy savings in buildings.* Energy Conversion and Management, 2001. **42**(11): p. 1307-1315.
22) Al-Sanea, S.A., *Thermal performance of building roof elements.* Building and Environment, 2002. **37**(7): p. 665-675.
23) Ascione, F., et al., *Green roofs in European climates. Are effective solutions for the energy savings in air-conditioning?* Applied Energy, 2013. **104**: p. 845-859.
24) Ouldboukhitine, S.-E., et al., *Assessment of green roof thermal behavior: A coupled heat and mass transfer model.* Building and Environment, 2011. **46**(12): p. 2624-2631.
25) Zinzi, M. and S. Agnoli, *Cool and green roofs. An energy and comfort comparison between passive cooling and mitigation urban heat island techniques for residential buildings in the Mediterranean region.* Energy and Buildings, 2012. **55**: p. 66-76.
26) Zingre, K.T., M.P. Wan, and X. Yang, *A new RTTV (roof thermal transfer value) calculation method for cool roofs.* Energy, 2015. **81**: p. 222-232.
27) Santamouris, M., A. Synnefa, and T. Karlessi, *Using advanced cool materials in the urban built environment to mitigate heat islands and improve thermal comfort conditions.* Solar Energy, 2011. **85**(12): p. 3085-3102.
28) Al-Homoud, D.M.S., *Performance characteristics and practical applications of common building thermal insulation materials.* Building and Environment, 2005. **40**(3): p. 353-366.
29) Halwatura, R.U. and M.T.R. Jayasinghe, *Thermal performance of insulated roof slabs in tropical climates.* Energy and Buildings, 2008. **40**(7): p. 1153-1160.
30) Hui, S.C. *Overall thermal transfer value (OTTV): how to improve its control in Hong Kong*. in *Proc. of the One-day Symposium on Building, Energy and Environment*. 1997.
31) Yao, R., B. Li, and K. Steemers, *Energy policy and standard for built environment in China.* Renewable Energy, 2005. **30**(13): p. 1973-1988.
32) Wong, N.H., et al., *The effects of rooftop garden on energy consumption of a commercial building in Singapore.* Energy and Buildings, 2003. **35**(4): p. 353-364.
33) Fioretti, R., et al., *Green roof energy and water related performance in the Mediterranean climate.* Building and Environment, 2010. **45**(8): p. 1890-1904.
34) Parizotto, S. and R. Lamberts, *Investigation of green roof thermal performance in temperate climate: A case study of an experimental building in Florianópolis city, Southern Brazil.* Energy and Buildings, 2011. **43**(7): p. 1712-1722.
35) Lazzarin, R.M., F. Castellotti, and F. Busato, *Experimental measurements and numerical modelling of a green roof.* Energy and Buildings, 2005. **37**(12): p. 1260-1267.
36) Akbari, H., S. Konopacki, and M. Pomerantz, *Cooling energy savings potential of reflective roofs for residential and commercial buildings in the United States.* Energy, 1999. **24**(5): p. 391-407.
37) Sproul, J., et al., *Economic comparison of white, green, and black flat roofs in the United States.* Energy and Buildings, 2014. **71**: p. 20-27.
38) Synnefa, A., M. Santamouris, and H. Akbari, *Estimating the effect of using cool coatings on energy loads and thermal comfort in residential buildings in various climatic conditions.* Energy and Buildings, 2007. **39**(11): p. 1167-1174.
39) Akbari, H., R. Levinson, and L. Rainer, *Monitoring the energy-use effects of cool roofs on California commercial buildings.* Energy and Buildings, 2005. **37**(10): p. 1007-1016.
40) Bakos, G.C., *Insulation protection studies for energy saving in residential and tertiary sector.* Energy and Buildings, 2000. **31**(3): p. 251-259.
41) M. Sanjay, P.C., *Passive cooling techniques in buildings: past and present - a review.* ARISER, 2008. **4**: p. 37–46.
42) Kolokotsa, D., et al., *Numerical and experimental analysis of cool roofs application on a laboratory building in Iraklion, Crete, Greece.* Energy and Buildings, 2012. **55**: p. 85-93.
43) Crawley, D.B., et al., *Energy plus: energy simulation program.* ASHRAE journal, 2000. **42**(4): p. 49-56.
44) EnergyPlus Weather Dataset, *Typical meteorological year weather data files for EnergyPlus simulations, U. S. Department of Energy*, University of Illinois, 2013, from http://apps1.eere.energy.gov/buildings/energyplus/weather data_about.cfm. (retrieved April 2013)
45) EnergyPlus Material Dataset, *The material data from EnergyPlus simulations, U. S. Department of Energy, University of Illinois, 2013*, from http://apps1.eere.energy. gov/buildings /energyplus/energyplus_documentation.cfm. (retrieved April 2014)
46) Sailor, D.J., *A green roof model for building energy simulation programs*. Energy and Buildings, 2008. **40**: p. 1466-1478.
47) ASHRAE. ASHRAE *handbook—fundamentals*, Atlanta: ASHRAE; 2009.
48) International Organization for Standardization, *ISO International 19840-12: Paints and varnishes—Corrosion protection of steel structures by protective paint systems—Measurements of, and acceptance criteria for, the thickness of dry films on rough surfaces*, Switzerland, 2012.
49) Kipp and Zonen, *CMP 11 Pyranometer Manual*, from http://www.kippzonen.com/Product/13/CMP-11-Pyranometer#.Unzcc-LcGhU.

50) American Society for Testing and Materials, *ASTM International C1549-09: Standard test method for determination of solar reflectance near ambient temperature using a portable solar reflectometer*, West Conshohocken, PA, 2009.
51) American Society for Testing and Materials, *ASTM International E408-13: Standard test method for total normal emittance of surfaces using inspection-meter techniques*, West Conshohocken, PA, 2013.
52) MadgeTech, *TransiTemp-II Manual*, from http://www.dalotech.com/madgetech/temperature/transitemp-II.php. (retrieved January 2014)
53) Scientific Sales Inc. *WeatherHawk 916 Manual*, from http://www.weatherhawk.com/documents/signature-series-specs.pdf. (retrieved January 2014)